The linker-loop region of *Escherichia coli* chaperone Hsp31 functions as a gate that modulates high-affinity substrate binding at elevated temperatures

M. S. R. Sastry*, Paulene M. Quigley†‡, Wim G. J. Hol†§, and François Baneyx*¶

Departments of *Chemical Engineering and †Biochemistry and §Howard Hughes Medical Institute, University of Washington, Seattle, WA 98195

Communicated by Earl W. Davie, University of Washington, Seattle, WA, April 29, 2004 (received for review December 12, 2003)

Precise control of substrate binding and release is essential for molecular chaperones to exert their protective function in times of stress. The mechanisms used are diverse and have been difficult to unravel. *Escherichia coli* heat-shock protein 31 (Hsp31) is a recent addition to the known complement of eubacterial chaperones. Crystallographic studies have revealed the presence of a hydrophobic bowl at the Hsp31 dimer interface and shown that the linker region connecting the two structural domains within each subunit is disordered. Together with a neighboring flexible loop, the linker caps a hydrophobic area adjacent to the bowl. Using a collection of Hsp31 mutants, we show that although both bowl and linker-loop-shielded residues participate in substrate binding, the latter are critical for protein capture at high temperature. Linker immobilization via an artificial disulfide bridge abolishes chaperone activity at elevated temperatures by precluding exposure of the underlying hydrophobic domain. We conclude that Hsp31 uses its linker-loop region as a thermally activated gate to control nonnative protein annealing to a high-affinity substrate-binding site. This simple yet efficient strategy to capture partially folded proteins under heat-shock conditions may be shared by other folding modulators.

molecular chaperones | heat-shock proteins | structure function | YedU | HchA

Molecular chaperones are a class of proteins that assist *de novo* folding and help prevent protein misfolding and aggregation in the cellular milieu (1). Chaperones typically bind hydrophobic stretches of amino acids exposed by (un)folding intermediates to the solvent by making use of structured hydrophobic patches present on their surface. To promote survival and maintain homeostasis of stressed cells, molecular chaperones must capture and release their substrates in a precisely timed fashion. How these events are controlled by conformational changes has only been elucidated in a small number of cases (1–5).

Escherichia coli Hsp31 is a homodimeric heat-shock protein (Hsp) that was identified originally by transcriptome analysis of thermally stressed cells (6) and later found to exhibit chaperone activity (7, 8). Highly conserved orthologs are present in a number of pathogens (8), and Hsp31 shares structural homology with archaebacterial PfpI-type peptidases (9) and with human DJ-1, a protein implicated in late-onset Parkinson's disease and male infertility (10–14). Although each Hsp31 monomer contains a poorly solvent-accessible catalytic triad (9, 12, 15, 16), the physiological relevance of this feature remains unclear because Hsp31 exhibits exceedingly weak protease activity against large protein substrates and only cleaves small single amino acids conjugated to a fluorogenic reporter (12). On the other hand, genetic evidence suggests that Hsp31 functions as a modified holding chaperone that helps the DnaK-DnaJ-GrpE system manage protein misfolding under severe thermal stress conditions (17).

Although *E. coli* Hsp31 suppresses the aggregation of model proteins *in vitro* and promotes their refolding from the chemically and thermally denatured states (7, 8), its mechanism of action remains unknown. The Hsp31 structure indicates that each 31-kDa subunit consists of two α-β domains termed A and P that are connected by a 22-residue-long linker extending from Gln-28 to His-49 and exhibiting high B-factors (9, 15). The largest hydrophobic surface feature of Hsp31 is a shallow bowl located at the P domain dimerization interface. It is ≈20 Å in diameter and involves seven residues from each subunit (Fig. 1*A*). We and others (9, 12, 16) have proposed that the Hsp31 bowl may be implicated in substrate binding. However, biochemical evidence suggests that high temperatures lead to the exposure of additional hydrophobic patches to the solvent (8). A recent crystal structure of *E. coli* Hsp31 has revealed that the linker and an adjacent loop extending from Met-103 to Lys-115 are disordered and mask 19 nonpolar residues, the display of which to the solvent increases the percentage of exposed hydrophobic area by 3% per monomer (9). In this work we used a combination of site-directed mutagenesis and disulfide cross-linking to probe the role of bowl and linker-loop-shielded residues in Hsp31 substrate binding. Results show that thermally induced motion of the flexible linker-loop region leads to the uncovering of a high-affinity substrate-binding site that is essential for Hsp31 to capture nonnative proteins at high temperatures.

Materials and Methods

Construction of Hsp31 Mutants. An N-terminal hexahistidine-tagged variant of Hsp31 was generated by PCR amplification of the *hchA* gene by using primers 5′-ATAAGGAAGGGCATATGACTGTTCAAACAAG-3′ and 5′-TTACATTCAAACCTCGAGGGGATTAACCCGCGTA-3′ and MC4100 genomic DNA. The amplified fragment was digested with *Nde*I and *Xho*I and cloned in the same sites of pET28a+ (Novagen) to yield pNT-hchA. Mutations were introduced on this plasmid by using the QuikChange site-directed mutagenesis kit (Stratagene) and the primers listed in Table 1.

Protein Purification. BL21(DE3) cells (Novagen) harboring the various Hsp31 expression plasmids were grown at 37°C in 250 ml of LB medium supplemented with 50 μg/ml neomycin. Cultures were induced with 1 mM isopropyl β-D-thiogalactoside at $A_{600} \approx 0.4$ and incubated to $A_{600} \approx 4.0$. Cells were sedimented by centrifugation at 8,000 × *g* for 10 min, resuspended in 50 mM sodium phosphate, pH 8.0, and disrupted with a French press at 10,000 psi (1 psi = 6.89 kPa). Insoluble material was removed by centrifugation at 15,000 × *g* for 15 min. Imidazole (35 mM) and NaCl (300 mM) were added to the supernatant, which was

Abbreviations: Hsp, heat-shock protein; MDH, malate dehydrogenase; ADH, alcohol dehydrogenase; CD, circular dichroism; CM, carboxymethylated; RCM, reduced carboxymethylated; ANS, 1-anilino-8-naphtalenesulfonate; Gdn·HCl, guanidine hydrochloride; CS, citrate synthase.

‡Present address: Targeted Genetics Corp., 1100 Olive Way, Suite 100, Seattle, WA 98101.

¶To whom correspondence should be addressed. E-mail: baneyx@u.washington.edu.

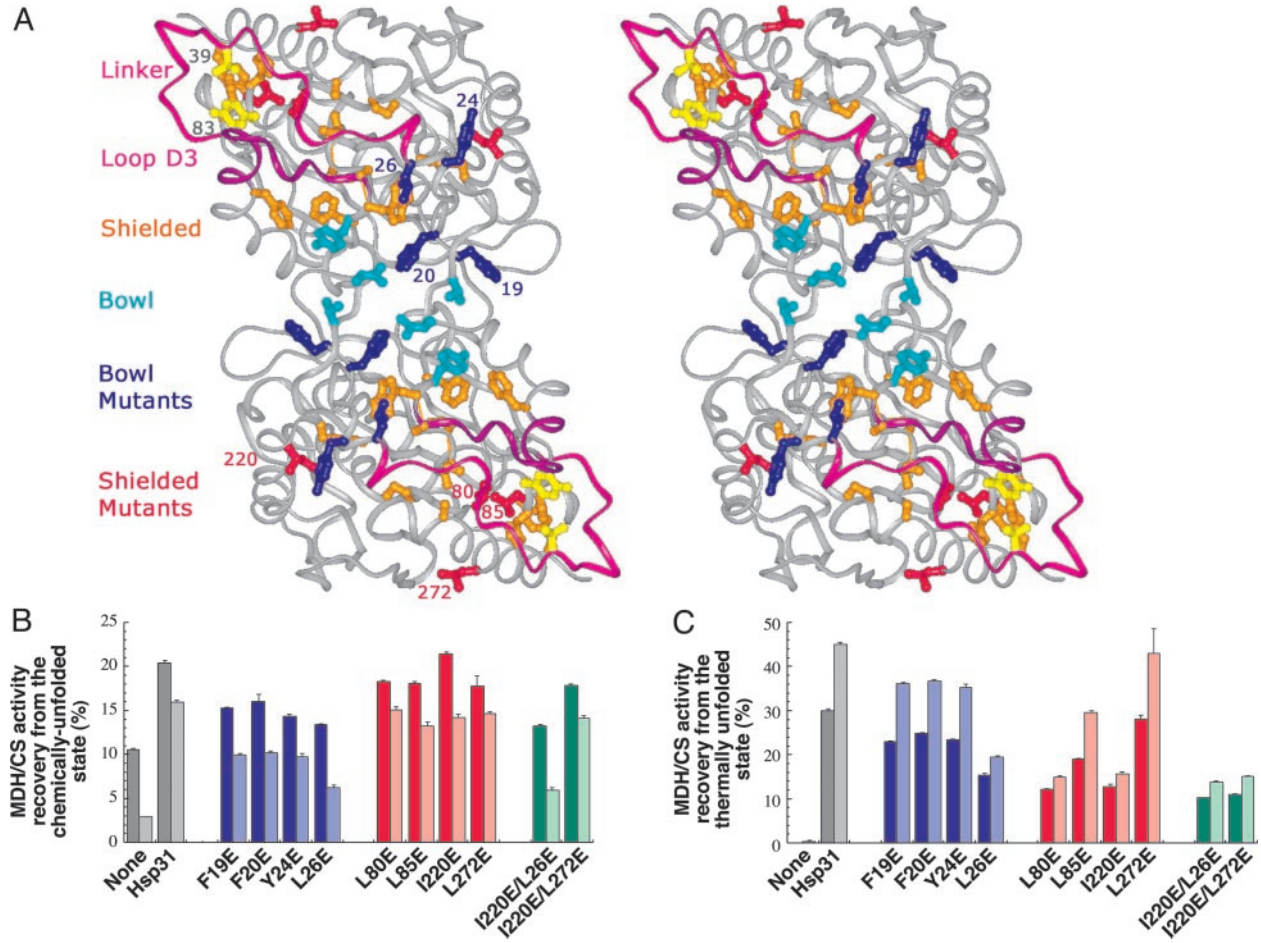

Fig. 1. Effect of glutamate substitutions in bowl and linker-loop-shielded residues on Hsp31 chaperone activity. (*A*) Stereoview of Hsp31 with bowl residues shown in cyan and blue (mutated residues) and linker-loop-shielded residues shown in orange and red (mutated residues). The linker (pink), loop (purple), and residues converted to cysteines (yellow) are shown also. (*B*) Gdn·HCl-unfolded MDH (dark bars) or urea-unfolded CS (light bars) was diluted in buffer containing Hsp31 variants. Samples were assayed after 3 h (MDH) or 30 min (CS) of incubation at 23°C. (*C*) MDH (dark bars) or CS (light bars) were mixed with Hsp31 variants, incubated for 30 min at 45°C, and assayed after 30 min at 23°C. Enzymatic activities measured with Hsp31 bowl mutants are shown in two shades of blue. Those measured in the presence of Hsp31 variants mutated in linker-loop-shielded residues are shown in two shades of red. Activity results for double mutants are shown in two shades of green. Error bars were obtained for three independent replicates of activity measurements that were each performed in triplicate.

loaded onto a 10-ml Ni^{2+}-nitrilotriacetic acid column (Qiagen, Valencia, CA). Bound proteins were eluted in 30 ml of phosphate buffer containing 300 mM NaCl and 250 mM imidazole. Samples were dialyzed for 24 h at 4°C against 100 mM Tris·HCl, pH 7.5. Hexahistidine tags were removed by incubating the samples with 300 μl of thrombin agarose (Sigma) for 6 h at room temperature followed by extensive dialysis against 100 mM Tris·HCl, pH 7.5. Complete removal of the tag was confirmed by immunoblotting with anti-His-6 antibodies (Novagen). Purity was >97%. Protein concentrations were determined by using the Coomassie dye-binding protein assay kit (Sigma). The extraneous N-terminal tripeptide (Gly-Ser-His) had no impact on chaperone activity as judged by malate dehydrogenase (MDH) refolding assays and alcohol dehydrogenase (ADH) aggregation-suppression experiments (M.S.R.S. and F.B., unpublished data). The structural integrity of all mutants was confirmed by gel-filtration chromatography, circular dichroism (CD) spectroscopy, and intrinsic tryptophan fluorescence at 23°C. Two linker-loop-shielded mutants, L79E and A88E, were found to exhibit altered secondary structure by CD spectroscopy and were not considered further. Mutant thermostability was verified by repeating CD and intrinsic tryptophan fluorescence measurements at 45°C. The only structural change observed was a 3-nm blue shift in the intrinsic tryptophan fluorescence spectrum of the F20E variant at both 23°C and 45°C. All other variants including single and double cysteine substitution mutants behaved as the wild type at both temperatures.

Protein Modification. The V39C/Y83C double mutant was carboxymethylated (CM) with iodoacetic acid (Sigma) as described (18). Briefly, 1 mg/ml of protein in 100 mM Tris·HCl, pH 8.2, was incubated in the presence or absence of 10 mM DTT at 37°C for 30 min. Iodoacetic acid (20 mM) was added, and samples were held in the dark at 23°C for 25 min and extensively dialyzed against the same buffer or against 100 mM sodium phosphate, pH 7.3, for Ellman assays. Determination of the free thiol content was performed as described (19).

Bis-1-anilino-8-naphtalenesulfonate-Binding Assays. Samples (0.8 μM) of native Hsp31, V39C, and Y83C variants and of the oxidized, CM, and reduced CM (RCM) forms of the V39C/Y83C double mutant were preincubated at 45°C for 5 min in 1 ml of 150 mM Tris·HCl, pH 7.5/10 mM KCl/5 mM $MgCl_2$. Bis-1-anilino-8-naphtalenesulfonate (ANS) (12 μM; Molecular Probes) was added to the samples at time 0. Fluorescence emission intensities after excitation at 340 nm were recorded at

Table 1. Primers used for the construction of Hsp31 mutants

Mutation	Primer set
F19E	5′-GAAGATAATGCAGAATTCCCTTCAGAA-3′
	5′-TTCTGAAGGGAATTCTGCATTATCTTC-3′
F20E	5′-GATAATGCATTCGAACCTTCAGAAT-3′
	5′-ATTCTGAAGGTTCGAATGCATTATC-3′
Y24E	5′-CCCTTCAGAAGAATCGCTTAGCCAA-3′
	5′-TTGGCTAAGCGATTCTTCTGAAGGG-3′
L26E	5′-CAGAATATTCGGAAAGCCAATATACC-3′
	5′-GGTATATTGGCTTTCCGAATATTCTG-3′
L80E	5′-TTGAAACGTTGGAACCGTTGTATCA-3′
	5′-TGATACAACGGTTCCAACGTTTCAA-3′
L85E	5′-CCGTTGTATCATGAACATGCTGCAGGT-3′
	3′-ACCTGCAGCATGTTCATGATACAACGG-5′
I220E	5′-AAACGCCAGAGGAAGGCTATATGCCG-3′
	5′-CGGCATATAGCCTTCCTCTGGCGTTT-3′
L272E	5′-CGTTGGGTAAAGAAGCGGCGCAGG-3′
	5′-CCTGCGCCGCTTCTTTACCCAACG-3′
Y83C	5′-GCTGCCGTTGTGTCATCTCCATGC-3′
	5′-GCATGGAGATGACACAACGGCAGC-3′
V39C	5′-TCTTGATGGCTGCGACTATCCAA-3′
	5′-TTGGATAGTCGCAGCCATCAAGA-3′

477 nm on a Hitachi (Tokyo) F-4500 spectrophotometer fitted with a thermostated cell held at 45°C. For control experiments, native Hsp31, the V39C and Y83C variants, and the oxidized V39C/Y83C double mutant were preincubated at 23°C for 5 min, and bis-ANS was added at time 0. Fluorescence emission intensities were recorded as described above except that the cell was held at 23°C.

Chaperone Activity Assays. The ability of Hsp31 variants (2.4 μM based on protomers) to support the reactivation of MDH (0.4 μM) from the guanidine hydrochloride (Gdn·HCl)-unfolded state or that of citrate synthase (CS) (0.4 μM) from the urea-unfolded state was determined after 3 h (MDH) or 30 min (CS) of incubation at room temperature as described (7, 8). Reactivation yields do not increase after these time periods. The ability of Hsp31 variants (2.4 μM) to support the reactivation of MDH (0.4 μM) or CS (0.4 μM) denatured by 30 min of incubation at 45°C was determined 30 min after transfer of the reaction mixtures to 23°C as described (8). All samples were assayed in triplicate, and error bars were obtained for three independent experiments. ADH (0.4 μM) aggregation-suppression experiments by Hsp31 variants (1.2 μM) at 41.5°C were conducted as described (8).

Results and Discussion

Hsp31 Mutagenesis. To assess the role of Hsp31 hydrophobic regions in substrate binding, we replaced four residues contributing to the architecture of the bowl and four nonpolar amino acids predicted to become solvent-exposed after linker-loop movement (hereafter referred to as linker-loop-shielded residues) by glutamate (Fig. 1*A*). All residues targeted for mutagenesis are 100% conserved in class I Hsp31 homologs (8, 9). The structural integrity and thermostability of the mutants were verified by gel-filtration, CD spectroscopy, and intrinsic tryptophan fluorescence measurements at both 23°C and 45°C. With the exception of F20E, the intrinsic tryptophan fluorescence spectrum of which exhibited a 3-nm blue shift relative to Hsp31, all variants behaved similarly to the native protein at both temperatures. We previously reported that Hsp31 supplementation doubles the recovery yields of active MDH after dilution from the Gdn·HCl-unfolded state at 23°C and that, although MDH is completely inactivated after 30 min of incubation at 45°C, addition of Hsp31 allows recovery of 30% of the original activity (8). We reasoned that the use of these two refolding conditions with the collection of Hsp31 site-directed mutants would allow us to dissect the contribution of bowl and linker-loop-shielded residues on substrate binding at low and high temperatures.

Substrate Binding at Low Temperatures. Fig. 1*B* (dark-shaded bars) shows that the F19E, F20E, and Y24E bowl residue substitutions reduced the ability of Hsp31 to improve the folding of Gdn·HCl-denatured MDH at 23°C by 40–60%. The L26E substitution had the most deleterious effect, leading to an ≈70% decrease in activity recovery relative to native Hsp31. Mutations in linker-loop-shielded residues had less severe consequences, causing an ≈25% reduction or exerting no influence (I220E) on MDH recovery yields relative to native Hsp31. To determine whether the unfolding method or the identity of the substrate would affect these results, experiments were repeated with urea-unfolded CS. In agreement with MDH data, the F19E, F20E, and Y24E substitutions caused a 45–60% reduction in activity recovery relative to native Hsp31, L26E had the most significant effect with a 75% decrease in yields, and mutations in linker-loop-shielded residues led to a 10–20% reduction in CS activity recovery (Fig. 1*B*, light-shaded bars). We therefore conclude that bowl residues play a dominant role in substrate binding at 23°C.

Substrate Binding at Elevated Temperatures. When we tested the ability of the various mutants to increase the recovery of active MDH or CS after thermal unfolding at 45°C, the situation was reversed (Fig. 1*C*). Three of four mutations in bowl residues (F19E, F20E, and Y24E) led to an ≈20% reduction in the recovery of active enzymes relative to native Hsp31, whereas two linker-loop-shielded mutants (L80E and I220E) caused a 60–65% loss in activity and a third (L85E) caused an ≈35% decrease in yields. As observed in the case of chemically unfolded substrates, the L26E mutation had the most deleterious effect among all bowl mutants tested (50–60% decrease in yields), whereas the L272E substitution had the smallest impact on Hsp31 chaperone activity. To confirm that the observed differences were related to deficiencies in substrate binding and to generalize results to a third model protein, aggregation-suppression experiments were conducted with the set of Hsp31 variants by using ADH as a substrate. There was very good agreement between the ability of both bowl (Fig. 2*A*) and linker-loop-shielded (Fig. 2*B*) mutants to inhibit ADH aggregation at 41.5°C and their capacity to promote the folding of active MDH or CS after incubation at 45°C (compare Figs. 1*C* and 2).

The fact that the L85E mutation exerts a less pronounced effect than the L80E or I220E substitutions in the experiments of Figs. 1*C* and 2*B* is consistent with the poor solvent accessibility of this residue compared with that of Leu-80 or Ile-220 (Fig. 1*A*). It therefore is likely that Leu-85 stabilizes rather than mediates substrate binding under heat-shock conditions. Furthermore, Leu-272 does not seem to play a central role in high-temperature substrate binding, because the L272E mutant behaved comparably to authentic Hsp31 with all model proteins and this substitution did not significantly aggravate the refolding defects of the I220E variant (Fig. 1*C*). In agreement with these results, Leu-272 is located at the periphery of the linker-loop-shielded hydrophobic patch (Fig. 1*A*). Interestingly, the bowl residue Leu-26 is a strong contributor to Hsp31 chaperone activity at both low and high temperatures. In light of the facts that Leu-26 is proximal to the origin of the linker (Fig. 1*A*) and that the effects of the I220E and L26E substitutions are not additive at elevated temperatures (Fig. 1*C*), the glutamate substitution at position

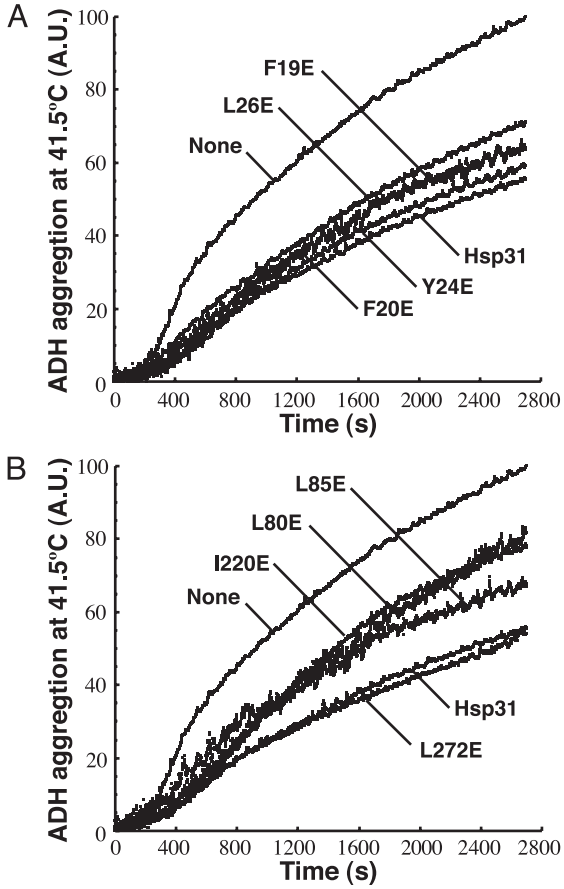

Fig. 2. Effect of glutamate substitutions in bowl and linker-loop-shielded residues on substrate binding. ADH thermal aggregation at 41.5°C was monitored by right-angle light scattering in the presence of Hsp31 variants mutated in bowl (*A*) or linker-loop-shielded (*B*) residues. Results are reported in arbitrary units (A.U.).

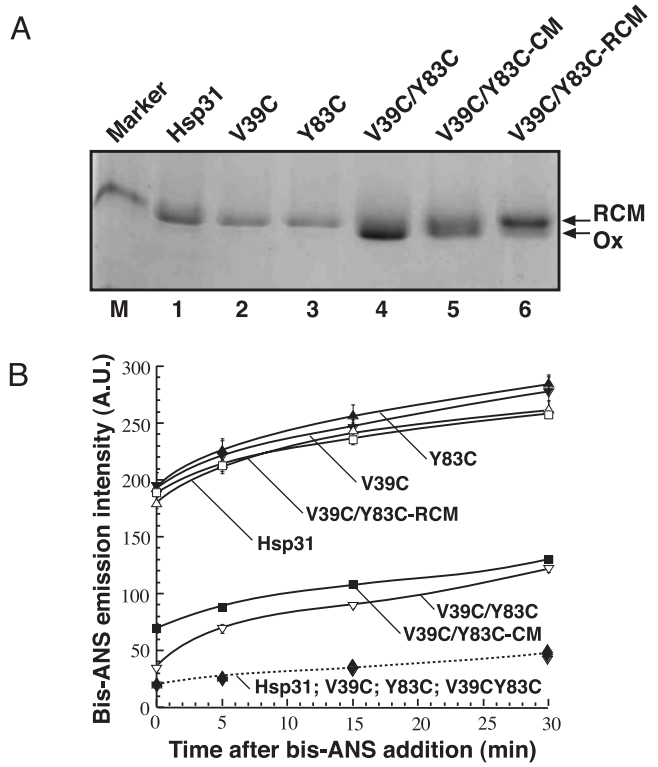

Fig. 3. Linker immobilization by an artificial disulfide connecting V39C to Y83C interferes with the temperature-driven exposure of structured hydrophobic domains. (*A*) Mobility of native Hsp31, single cysteine mutants, and the oxidized (Ox), CM, and RCM versions of the cysteine double mutant on a nonreducing SDS gel. Lane M contains a 36-kDa marker. (*B*) Solid lines, the three forms of the double cysteine mutant along with native Hsp31 and the V39C and Y83C single mutants were preincubated at 45°C for 5 min and supplemented with bis-ANS at time 0, and bis-ANS emission intensities were recorded after the indicated incubation times at 45°C; dashed line, native Hsp31, the V39C and Y83C variants, and oxidized V39C/Y83C were preincubated at 23°C for 5 min and supplemented with bis-ANS at time 0, and bis-ANS emission intensities were recorded after the indicated incubation times at 23°C. Symbols overlap. Note that emission intensities at 23°C and 45°C cannot be compared directly because of the different quantum yield of the reporter at the two temperatures. Error bars correspond to triplicate experiments, and results are reported in arbitrary units (A.U.).

26 is likely to affect linker-loop mobility. In summary, the data discussed above indicate that both hydrophobic domains are implicated in Hsp31 chaperone function and that the role of linker-loop-shielded residues in substrate binding becomes more critical as the temperature increases.

Disulfide Cross-Linking of the Linker-Loop Region. To further probe the contribution of the linker-loop region and the role of its predicted mobility in substrate-binding events, we replaced the central linker residue Val-39 (50% conserved in class I Hsp31 orthologs) and a proximal linker-shielded residue of the A domain (Tyr-83; 83% conserved in class I orthologs) by cysteines. These locations were inferred from structural data with the expectation that formation of a disulfide bridge would immobilize both linker and loop onto the protein core because their movement appears to be coupled (9).

The purified double mutant exhibited a faster electrophoretic mobility on nonreducing gels relative to either native Hsp31 or the V39C or Y83C variants, as would be expected if a disulfide bond had formed as a result of air oxidation (Fig. 3*A*, lanes 1–4). Ellman assays confirmed the presence of 2.07 free thiols (corresponding to native Cys-185 and Cys-207) in the V39C/Y83C mutant, compared with 4.23 free thiols after DTT reduction. Furthermore, reductive carboxymethylation of the double mutant reduced electrophoretic mobility relative to its oxidized counterpart or to a CM control prepared in the absence of reducing agent (Fig. 3*A*, lanes 4–6). The smear of intermediate mobility species observed with the latter sample likely corresponds to differential carboxymethylation products of the two deeply buried cysteines present in authentic Hsp31. Finally, gel-filtration, CD spectroscopy, and intrinsic tryptophan fluorescence experiments revealed that the V39C, Y83C, and V39C/Y83C mutants behaved as native Hsp31 at both 23°C and 45°C (data not shown). We conclude that a disulfide bridge spontaneously forms in the V39C/Y83C variant and it does not significantly affect Hsp31 structure or thermostability.

Linker-Loop Immobilization Abolishes Hsp31 Chaperone Activity at High Temperatures. To assess the effect of the Cys-39/Cys-83 disulfide on the temperature-driven exposure of linker-loop-shielded hydrophobic domains to the solvent (8), Hsp31 variants were preincubated at 45°C for 5 min and supplemented with bis-ANS. This small reporter molecule exhibits little fluorescence in its free state but becomes highly fluorescent when bound to structured hydrophobic patches. Fig. 3*B* (solid lines) shows that the bis-ANS emission intensity of the RCM double mutant was comparable with that of native Hsp31 as well as that of the V39C and Y83C single mutants. By contrast, the emission intensity at 477 nm was ≈2.5-fold lower for the oxidized forms

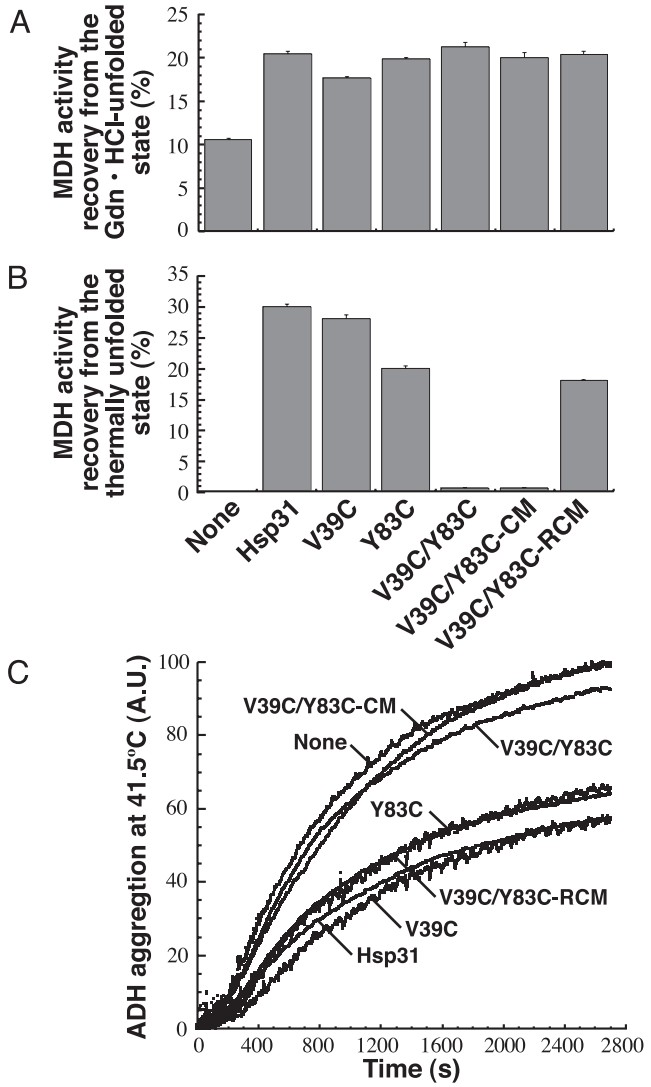

Fig. 4. Linker mobility is essential for Hsp31 substrate binding at high temperatures. (*A*) Gdn·HCl-unfolded MDH was diluted into buffer containing Hsp31, the single cysteine mutants, or the three forms of the double cysteine mutant. Samples were assayed after 3 h at 23°C. (*B*) MDH was mixed with Hsp31 variants, incubated 30 min at 45°C, and assayed after 30 min at 23°C. Error bars were obtained for three independent replicates of activity measurements that were each performed in triplicate. (*C*) ADH thermal aggregation was monitored by light scattering in the presence of the indicated Hsp31 variants. Results are reported in arbitrary units (A.U.).

of the V39C/Y83C variant. In control experiments performed at 23°C, there was little difference in bis-ANS emission intensities between Hsp31, V39C, Y83C, and oxidized V39C/Y83C (Fig. 3*B*, dashed line). Thus, although it has no effect on Hsp31 surface hydrophobicity at low temperatures, the disulfide bridge connecting Cys-39 to Cys-83 efficiently precludes the exposure of nonpolar residues at 45°C, most likely by restricting linker-loop mobility.

We observed little difference in recovery yields when the chaperone activity of the Hsp31 cysteine variants was tested with Gdn·HCl-unfolded MDH (Fig. 4*A*) or urea-unfolded CS (data not shown), confirming that linker-loop-shielded residues do not play a critical role in substrate binding at low temperatures. Remarkably, however, the oxidized forms of the V39C/Y83C double mutant almost completely lost their ability to support MDH reactivation from the thermally denatured state (Fig. 4*B*). Similar results were obtained with heat-unfolded CS. Whereas the V39C and Y83C single mutants allowed recovery of 43.5% and 30.2% of the original CS activity, respectively (compared with 45% for native Hsp31), only 2.3% was recovered with the oxidized V39C/Y83C mutant. As expected from the activity data, neither oxidized V39C/Y83C nor its CM form was able to suppress ADH aggregation at 41.5°C (Fig. 4*C*). Furthermore, the Y83C mutant exhibited decreased activity in MDH/CS reactivation and ADH aggregation-suppression experiments, indicating that Tyr-83 contributes to the architecture of the binding site. Loss of substrate binding by the oxidized double mutant was directly related to linker immobilization, because chaperone function was restored to the level of the Y83C variant when experiments were repeated with the RCM form of the protein (Fig. 4 *B* and *C*).

Mechanistic Implications. Taken together, our data indicate that the plasticity of the Hsp31 linker-loop region plays a key role in modulating chaperone function at high temperatures by gating access to a high-affinity binding site and proves a mechanism of action inferred from structural data only (15). Under physiological conditions, certain nonnative proteins may bind to the hydrophobic bowl region of Hsp31. Although nonessential under balanced growth (17), such Hsp31-mediated partitioning of folding intermediates from the solvent could improve their folding via a mass-action effect. Under heat-shock conditions, the high B-factor linker-loop region should become highly mobile, resulting in the exposure of the previously shielded, underlying hydrophobic area. Unstructured and hydrophobic segments of folding intermediates may bind directly to this region or may interact first with the bowl and anneal to the high-affinity binding site. Taking into account the temperature-dependent increase in the strength of hydrophobic interactions, efficient substrate capture should ensue. As stress subsides, the linker would resume its original position and, in the process, eject the substrate in an environment permissive for folding.

It is likely that Hsp31 uses additional mechanisms to fine-tune substrate interactions. For instance, we previously reported that ATP binding negatively regulates Hsp31 chaperone activity at high temperatures by precluding the exposure of hydrophobic domains (8), and a Zn(II)-binding site proximal to the linker-loop region has been described recently (16). It will be of interest to determine whether and how nucleotide or metal binding affect linker-loop movement.

Regulation of substrate capture and release by conformational changes seems to be a common theme in chaperone mode of action. In the case of DnaK, precise control of binding and release events by two protein cofactors (DnaJ and GrpE) and adenosine nucleotides may be necessary for the chaperone to properly perform its multiple cellular functions, which range from *de novo* folding at physiological temperatures to protein disaggregation (20). Similarly, because it is an essential folding modulator at all temperatures (21), GroEL requires GroES and ATP-modulated conformational changes to efficiently promote substrate refolding at infinite dilution within its Anfinsen's cage (1). The mechanisms used by other chaperones may guarantee that they only become activated (or exhibit optimal function) under predetermined stress conditions. For instance, Hsp33, a conserved chaperone involved in the management of oxidative stress, uses a redox-sensitive Zn-coordinating cysteine center to control monomer dimerization and activation of chaperone activity (2). The *E. coli* periplasmic protein DegP (HtrA) relies on its postsynaptic density-95/DLG/ZO-1 (PDZ) domains and temperature-induced structural rearrangements to swap function from chaperone to protease as the temperature increases (4, 5). Finally, the *Saccharomyces cerevisiae* small heat-shock protein Hsp26 uses

temperature-induced dissociation from an oligomeric to a dimeric form to interact efficiently with its substrates (3). The thermal gate function of the flexible Hsp31 linker-loop region is a simple and efficient alternative to activate substrate binding under heat-shock conditions. This new paradigm may be shared by other folding modulators and illustrates the remarkable diversity of strategies that molecular chaperones have evolved to precisely regulate substrate interactions.

We thank Mirna Mujacic for critical reading of the manuscript. This work was supported by National Science Foundation Award BES-9707729 and National Institutes of Health Grant CA65656.

1. Hartl, F. U. & Hayer-Hartl, M. (2002) *Science* **295,** 1852–1858.
2. Graf, P. C. & Jakob, U. (2002) *Cell. Mol. Life Sci.* **59,** 1624–1631.
3. Haslbeck, M., Walke, S., Stromer, T., Ehrnsperger, M., White, H. E., Chen, S., Saibil, H. R. & Buchner, J. (1999) *EMBO J.* **18,** 6744–6751.
4. Krojer, T., Garrido-Franco, M., Huber, R., Ehrmann, M. & Clausen, T. (2002) *Nature* **416,** 455–459.
5. Spiess, C., Beil, A. & Ehrmann, M. (1999) *Cell* **97,** 339–347.
6. Richmond, C. S., Glasner, J. D., Mau, R., Jin, H. & Blattner, F. R. (1999) *Nucleic Acids Res.* **27,** 3821–3835.
7. Malki, A., Kern, R., Abdallah, J. & Richarme, G. (2003) *Biochem. Biophys. Res. Commun.* **301,** 430–436.
8. Sastry, M. S. R., Korotkov, K., Brodsky, Y. & Baneyx, F. (2002) *J. Biol. Chem.* **277,** 46026–46034.
9. Quigley, P. M., Korotkov, K., Baneyx, F. & Hol, W. G. J. (2003) *Proc. Natl. Acad. Sci. USA* **100,** 3137–3142.
10. Honbou, K., Suzuki, N. N., Horiuchi, M., Niki, T., Taira, T., Ariga, H. & Inagaki, F. (2003) *J. Biol. Chem.* **278,** 31380–31384.
11. Huai, Q., Sun, Y., Wang, H., Chin, L. S., Li, L., Robinson, H. & Ke, H. (2003) *FEBS Lett.* **549,** 171–175.
12. Lee, S. J., Kim, S. J., Kim, I. K., Ko, J., Jeong, C. S., Kim, G. H., Park, C., Kang, S. O., Suh, P. G., Lee, H. S., *et al.* (2003) *J. Biol. Chem.* **278,** 44552–44559.
13. Tao, X. & Tong, L. (2003) *J. Biol. Chem.* **278,** 31372–31379.
14. Wilson, M. A., Collins, J. L., Hod, Y., Ringe, D. & Petsko, G. A. (2003) *Proc. Natl. Acad. Sci. USA* **100,** 9256–9261.
15. Quigley, P. M., Korotkov, K., Baneyx, F. & Hol, W. G. J. (2004) *Protein Sci.* **13,** 269–277.
16. Zhao, Y., Liu, D., Kaluarachchi, W. D., Bellamy, H. D., White, M. A. & Fox, R. O. (2003) *Protein Sci.* **12,** 2303–2311.
17. Mujacic, M., Bader, M. W. & Baneyx, F. (2004) *Mol. Microbiol.* **51,** 849–859.
18. Creighton, T. E. (1989) in *Protein Structure: A Practical Approach*, ed. Creighton, T. E. (OIRL, Oxford), Vol. 7, pp. 155–167.
19. Ellman, G. L. (1959) *Arch. Biochem. Biophys.* **82,** 70–77.
20. Dougan, D. A., Mogk, A. & Bukau, B. (2002) *Cell. Mol. Life Sci.* **59,** 1607–1616.
21. Fayet, O., Ziegelhoffer, T. & Georgopoulos, C. (1989) *J. Bacteriol.* **171,** 1379–1385.